



Experimental Investigation of Friction Pressure Influence on the Characterizations of Friction Welding Joint for AISI 316

A. Jabbar Hassan^{*a}, T. Boukharouba^a, D. Miroud^b, N. Titouche^c, S. Ramtani^d

^a LMA, USTHB, BP. 32, El-Alia, 16111 Bab-Ezzouar, Algiers, Algeria

^b LSGM, USTHB, BP. 32; El-Alia, 16111 Bab-Ezzouar, Algiers, Algeria

^c DEMEM, DTN, Centre de Recherche Nucléaire de Birine, BP. 180, Ain Oussera, Djelfa, Algeria

^d CSPBAT – LBPS, UMR 7244 CNRS, Paris University 13, Galilée Institute, 99, J.B. Clément Street, Villetaneuse, France

PAPER INFO

Paper history:

Received 02 April 2020

Received in revised form 23 April 2020

Accepted 12 June 2020

Keywords:

Austenitic Stainless Steel

Friction Pressure

Hardness

Micro-hardness

Ultimate Tensile Strength

ABSTRACT

This study focuses on the effect of friction pressure on the welding joint strength of AISI 316. Single factor method was used to evaluate the influence of friction pressure, whilst the other conditions kept constant. The experimental data were achieved by temperature measurement using infrared thermometer and thermometer by touch, where hardness H_{V10} and micro-hardness $H_{V0.1}$ realized along the axial direction, tensile test specimen with 8 mm effective diameter, scanning electronic microscopy (SEM) to observe tensile fracture surface and x-ray diffraction (XRD) to analyze the concentration of gamma iron. The results by high friction pressure provide increased temperature during friction and forging phase, elevated hardness and micro-hardness values at the welding center, improved ductility and ultimate tensile strength (UTS). Whilst the central region of tensile fracture seemed most ductile mode and presence of micro-porosities with different forms and dimensions, hence concentration of face centered cubic (FCC) structure of gamma iron clearly revealed at level of 111.

doi: 10.5829/ije.2020.33.12c.12

1. INTRODUCTION

Austenitic stainless steel AISI 316 is used for various applications in chemical, manufacture of textile equipment, marine, and electrical appliance industries, etc. This type of steel is similar to AISI 304, but with addition of molybdenum to improve its resistance to pitting corrosion and resistance at high temperatures. Moreover, AISI 316 is easy to weld by fusion welding techniques, but it is preferred to avoid fusion welding due to phase transformations occurring in the welding and heat affected zones [1], also creating intermetallic compounds due to high amount of heat input [2], hence leading to loss of some useful original mechanical properties of the metal [3].

Considering all aspects, conditions and disadvantages, several studies have suggested replacing fusion welding by modern techniques such as friction

welding [4]. This technique is one of the solid state welding processes which provides welding below the melting temperature of the metal being joined. It is also subdivided mainly into two most prominent processes: direct drive [5-6] and friction stir [7-11]. The direct drive friction welding is a technique which creates joining by heat developed between contact surfaces under the effect of rotation speed and applied pressure, one of the parts is stationary whereas the other is rotating and the two still in contact with each other until rotation stops abruptly, where the pressure increases to complete welding joint. This technique is preferred because of sub-melting temperature, high reproducibility, and low input energy, easy and fast procedure with reduced formation of the inter-metallic compounds [6, 12].

Several researches have been reported the influence of the friction pressure on the properties of welding joint [13-14]. In general and according to earlier studies, friction pressure should be always kept high to obtain elevated strength of welding joint, because of low

*Corresponding Author Email: jabbarhassan1973@yahoo.fr
(A. Jabbar Hassan)

friction pressure rendering lack of bonding [15]. Friction pressure is a significant parameter in changing tensile strength and hardness followed by forging pressure and speed of rotation. Note that high friction pressure increases hardness and tensile strength due to higher friction pressure lead to more heat generation [16].

It is worthwhile to mention that some works explained the effect of temperature and thermal curve during friction welding process [14, 17-18]. Since the temperature in the welding center is low relative to the peripheral [19], H. Ma et al. [14] and E. P. Alves et al. [20] support the idea of measuring the temperature at the center. Therefore, the present study explains the relation between friction pressure and temperature measured in the welding center cause of this relation had a low importance in the previous articles. The welding temperature created from high friction pressure and rotation speed will determine the nature of forging, and that will affect the welding joint strength.

2. MATERIALS AND METHOD

The steel used in the current study is commercial austenitic AISI 316 stainless steel with Ref. No. 4401. The metal received as a long shaft of 6 m length and cut to small pieces, 45 mm length and 12 mm diameter. The general properties are shown in the tables below. Table 1 illustrates the chemical composition showing the amount of alloying elements added to the base metal. Tables 2 and 3 show the mechanical and physical properties of the parent metal, respectively.

TABLE 1. Alloying elements of base metal (spectrum, wt. %)

C	Mn	Si	P	S	Mo	Cr	Ni
0.070	1.500	0.670	0.030	0.021	2.93-3.00	17.93-18.00	9.95-10.00

TABLE 2. Mechanical properties of base metal (as received, Ref. No. 4401)

UTS (MPa)	Young's modulus (MPa)	Elongation (%)	Average micro-hardness (Hv _{0.1})	Average hardness (Hv ₁₀)
670 - 680	≈ 1.93 × 10 ⁵	≈ 45	260 - 265	203 - 206

TABLE 3. Physical properties of the test metal (as received, Ref. No. 4401)

Density (g/cm ³)	Specific heat (j/kg. °k) 0-100°C	Thermal conductivity (w/mk)	T. melting (°C)
8	5	16.00-16.20	1371-1400

Figure 1 explains the flow chart of procedure of friction welding steps, after initializing of the welding machine end effector and selects welding conditions, provide tests of temperature, mechanical and metallography to obtain the results and understand the behaviour of friction pressure influence on the joint strength. Figure 2 exposes the variation of friction welding conditions, that is friction and forging pressure during time of welding. It also shows evolution of flash during heating cycle under the effect friction and forging pressure.

The machine used in this study was designed and fabricated as a direct drive friction welding machine; it is controlled numerically by computer to examine the welding conditions. The machine is shown in Figure 3; its operating speed can be varied from 0 to 3000 rpm, and a maximum pressure of 300 MPa can be applied. Selection of the welding conditions were depending on the single factor method (Table 4) by changing one condition and keeping the others constant. This procedure was time consuming and required hard work, but achieved better vision on the performance of welding joint. Thus, there were other factors considered for the selected friction welding conditions, such as work-piece dimensions, nature of metal and refer to the previous researches [1, 6, 14-15, 19].

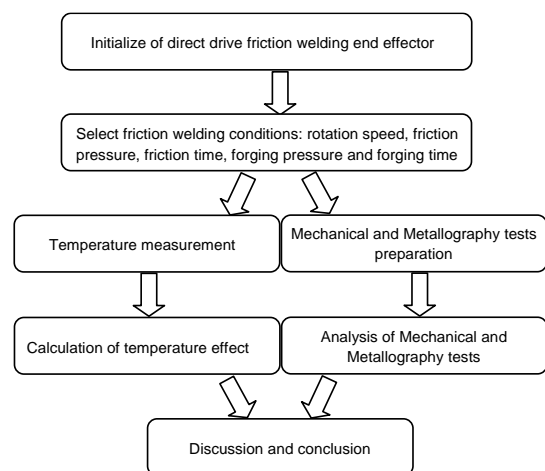


Figure 1. Flow chart of friction welding procedure

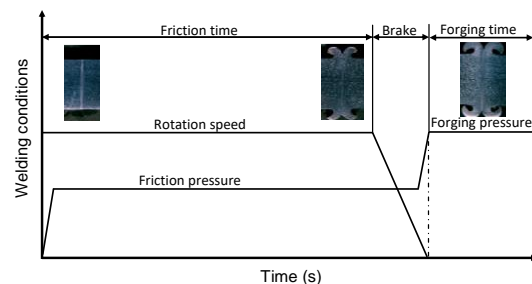


Figure 2. Diagram of direct drive friction welding conditions

Welding temperature recorded near the center of the interface of the stationary part (Figure 4). The temperature was recorded and verified by two methods as revealed in Figure 3, first one is thermometer by touch from type K with wire diameter of 0.5 mm and maximum temperature is 1400 °C (± 50°C), while second one is infrared thermometer (remote) from type K with maximum temperature is 1350 °C (± 50°C).

Scanning electronic microscopy (SEM) performed by JEOL JSM-6360 with magnifications of X 27 and X 150. X-ray diffraction (XRD), on the other hand, achieved by X'Pert PRO PANalytical. Whereas macroscopic observations were carried out by optical macroscopic from type NIKON SMZ 745T to measure the form of flash. SHIMADZU HMV testing machine were used in ambient temperature conditions for micro-hardness measurements in axial direction. While, The test pieces were polished with abrasive paper up to 1200 grit follow by 1 µm diamond paste on light disc cloth and oiled by ethanol and cleaned via deionized water.



Figure 3. Friction welding machine and the two thermometers, 1. welding machine; 2. Infrared thermometer (remote); 3. Thermometer by touch

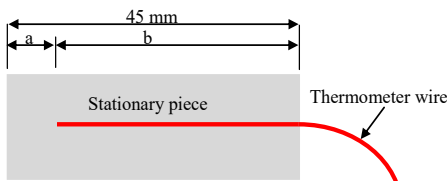


Figure 4. Thermometer by touch, position of the wire into the center of stationary piece, a: axial shortening + 0.5 mm; b: penetration distance of thermometer wire into center of stationary piece

TABLE 4. Friction welding conditions

Rotation speed (rpm)	Friction time (s)	Friction pressure (MPa)	Forging time (s)	Forging pressure (MPa)
		110		
3000	12	130	5	260
		150		
		170		

Vickers micro-hardness conditions were 100 gf load for 10 s. Whilst Vickers hardness test measurements achieved by INSTRON WOLPERT HARDNESS tester analyzed along the axial direction also, with 10 kg load applied for 10 s. The tensile tests were performed by using INSTRAN 5500 with 8 mm diameter under the standard of ISO 6892-1: 2009 (F).

3. RESULTS AND DISCUSSION

The thermal curves as shown in Figure 5 introduced the average values of temperature versus time. The rubbing between two pieces increased the temperature at the interface until reaches the maximum value (T_{max}), while the metal at that point still in the solid state. The created heat converted the solid metal to soft state, which is led to decreased the friction and that gradually reducing temperature. Under high rotation speed and pressure, the metal extruded from central to the peripheral to form flash metal. At the end of friction phase the rotation stops suddenly and the pressure increased at level of temperature which is called forging temperature (T_f) during forging phase period, this temperature has an important influence on the obtained welding joint.

The relation between T_{max} and T_f as shown in Figure 6 exposed that T_{max} regularly increased with higher friction pressure, the variation of maximum temperature between 793 °C - 1057 °C, that make clear of friction pressure elevation influences on the maximum temperature (T_{max}), hence forging temperature (T_f) roughly increased between 299 °C - 445 °C. In general, friction pressure has a direct proportional with T_{max} and T_f . Remarkable, with low friction pressure, the forging performed in low temperature and that consequently effected on the final properties of the joint.

The macroscopic observation as shown in Figure 7 represented the amount of flash formation of four friction pressures. Notes that with increasing friction

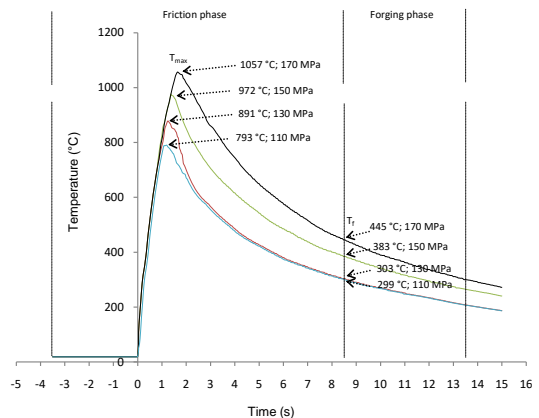


Figure 5. The thermal curves for the average values of temperatures versus time for different friction pressure

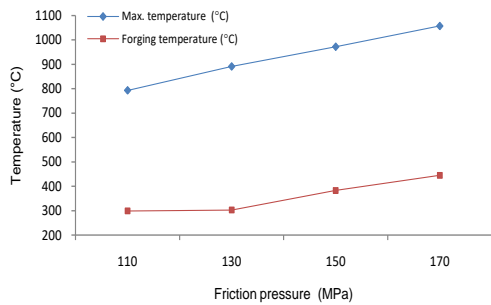


Figure 6. The relation between maximum temperature (T_{max}) and forging temperature (T_f) for different friction pressure

pressure; high amount of flash formation can be obtained [13, 15]. Obviously, Figure 8 reveals that increasing friction pressure elevated axial shortening, that because of increasing in friction pressure leads to rising T_{max} and T_f , which provide enough superheating and amplified the displaced metal from central to the peripheral under effect of friction pressure and rotation. The amount of flash formation depends on the mechanical properties of the metal being welded [21] such as hardness [22] also relies on the quantity of alloying elements and capability of thermo-plastic deformation [6], furthermore, presence of Cr, Ni and Mo provide stainless steel to be refractory, which requires more pressure and temperature during friction welding phases to obtain considerable amount of flash formation.

The hardness obtained along the axial direction (Figure 9) recorded the highest values at the welding interface, this increasing of hardness due to high friction pressure application [19]. While, shows falling of hardness when moving from central toward the base

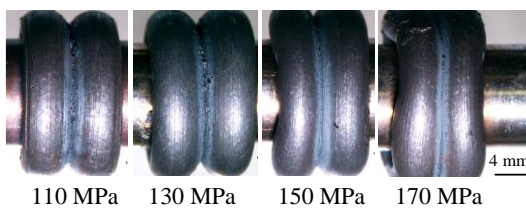


Figure 7. Flash formation for different friction pressure

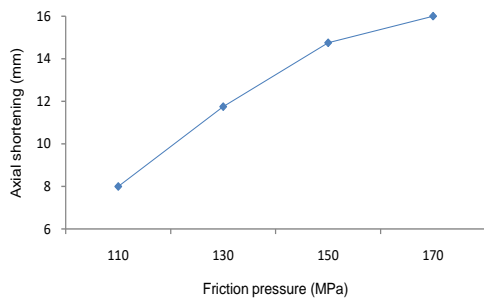


Figure 8. Axial shortening vs. friction pressure

metal, the increasing of hardness perhaps explained by the thermo-plastic deformation which exist in the interface resulting from dynamic recrystallisation, particularly at high friction pressure and temperature. P. M. AJITH et al. [16] agreed that with increasing friction pressure leads to high level of hardness at the interface due to dynamic recrystallization which results fine grains, there are also another source which is the high temperature at tangential area.

Micro-hardness profiles for axial direction as demonstrated in Figure 10, explain the effect of friction pressure has responsibility on the micro-hardness increasing of welding interface [13]. Moreover, due to high friction pressure with high rotation speed increased the superheated which produces dynamic recrystallisation. F.C. Liu, and T. W. Nelson [23] revealed that when the metal subjected to high plastic deformation under high temperature the dynamic recrystallisation occurs. On the other hand, the micro-hardness decreasing in the adjacent zone, due to amount of Mo. According to the alloying elements as shown in Table 1, AISI 316 has 2.93 % of Mo, that made the steel more refractory and led to reduce cooling rate speed and slow of heat diffusion causing decreasing micro-hardness at neighboring zone of welding joint [6].

Tensile test curves shown in Figure 11 illustrates the effect of friction pressure on the ultimate tensile

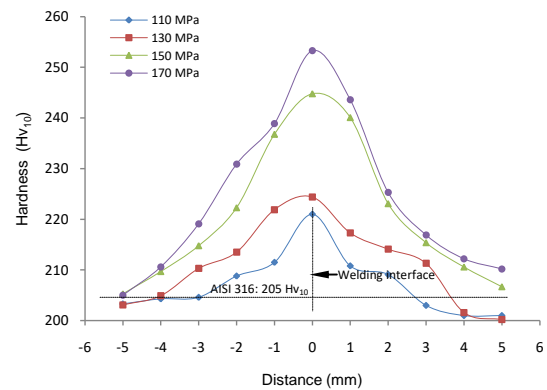


Figure 9. Hardness profile for axial direction

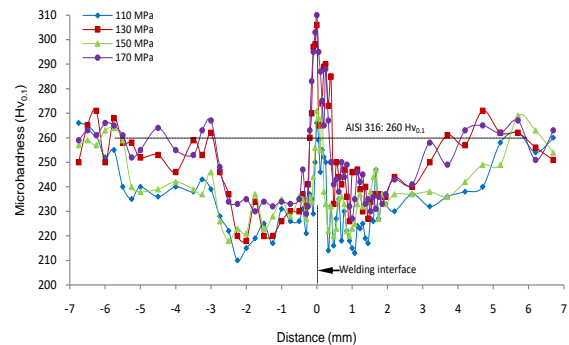


Figure 10. Micro-hardness profile for axial direction

strength (UTS) and ductility, the curves reveal also the values of UTS varied from 649 MPa to 667 MPa for friction pressure of 110 MPa to 170 MPa respectively, whilst ductility increased from 24 % to 29 % for friction pressure of 130 MPa to 170 MPa respectively. Explain this increasing of UTS and ductility by elevation of friction pressure because of thermo-plastic deformation in the bond line increases, which lead to more mass displaced at the interface [13]. I. Kirik and N. Ozdemir [21] exposed that high tensile strength was refer to more heat input and large plastic deformation at the interface under effect of high rotation speed. Moreover, rotation speed has important influence on the UTS, with high rotation speed UTS increases, while with low rotation exhibited a reverse trend, that because of heat generation elevates with high rotation speed. This phenomenon also observed in friction stir welding as mentioned in the references [10, 24]. Thus, the elevation of temperature at the two phases (friction and forging) has large consequence on the value of UTS and ductility. Finally, high friction pressure (170 MPa) and high rotation speed (3000 rpm) cause elevated temperature (1057 °C), that lead to high level of hardness and micro-hardness at the interface, and also elevation in UTS and ductility.

Figure 12 illustrated, on the other hand, the tensile specimens after tests, the figure exposed the position of fracture in the region close to the welding interface, elongation in the gauge length and the necking in the fracture position explained the amount of heat input at this region. In addition, the reduction in across sectional area (necking) provided more explanation about ductility than elongation of gauge length. Therefore, the

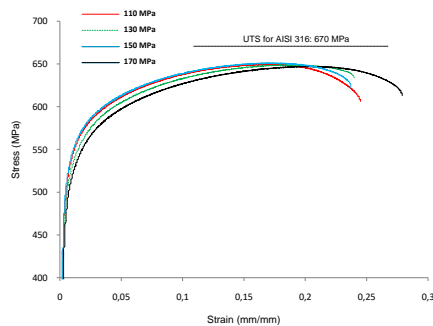


Figure 11. Curves of tensile tests for all welded joint relative to UTS of AISI 316

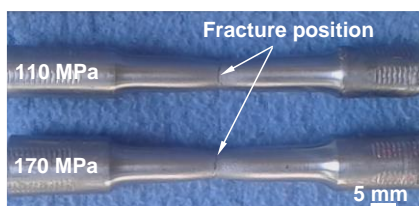


Figure 12. Macro-graphic of tensile test pieces

necking proved of ductility nature of fracture for 170 MPa more than in 110 MPa, this is also agreed with the tensile curves.

SEM observation for tensile fracture surface as shown in Figure 13 appears the spirals shape on the fracture surface for the friction pressure of 110 MPa and 170 MPa. The thermo-plastic deformation demonstrates by existing of that spirals shape on the fracture surface. Furthermore, the degree of thermo-plastic deformation seems according to the amount of spiral forms, while the phenomenon of spiral occurs due to metal flow neighboring of weld [6]. In addition, the result of aggressive friction pressure at elevated temperature and high rotation occurs that type of spiral forms. Whilst, magnification of central region of fracture seems most ductile mode with micro-porocities of different forms and dimensions. This mode of ductile fracture looks more clear at 170 MPa, which have the same opinion with the results of tensile curves as discussed earlier.

XRD analysis for friction pressure of 110 MPa and 170 MPa with compared to the base metal as shown in Figure 14. The concentration of FCC structure of gamma iron at level of 111 was evidently. This concentration gives explanation of thermo-plastic deformation due to thermomechanical strain because of high rotation speed under application of aggressive friction pressure. On the other side, the elevated temperature during process and nature of metal play major roles on the properties of welding joint. Additionally, amount of alloying elements, particularly

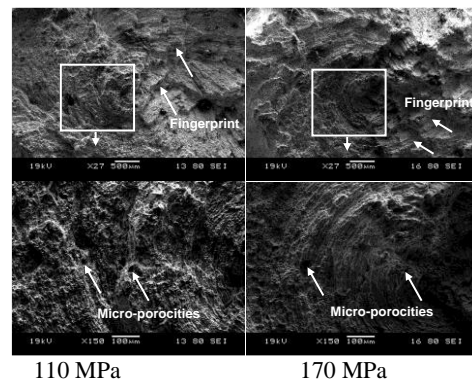


Figure 13. SEM observation for 110 MPa and 170 MPa

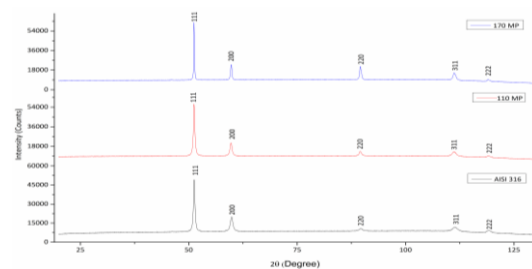


Figure 14. XRD analysis for 110 MPa, 170 MPa and AIS 316

Mo element effects on the quantity of heat diffusion or absorptions because of cooling rate that give Mo ability to effect on the phase attentiveness in the welding joint.

4. CONCLUSION

The effect of friction pressure on the evolution of the welding joint properties for AISI 316 summarized as following:

- Friction pressure has a direct proportional with maximum temperature (T_{max}) and forging temperature (T_f), that gives enough superheat which responsible on high amount of flash formation. On the other hand, with low friction pressure, the forging performed in low temperature and that consequently effected on the final propertie of welding joint,
- The hardness and micro-hardness variations recorded that the highest values at joint center, this elevation due to high friction pressure application. Whereas, shows falling of hardness and micro-hardness when moving from central toward the base metal,
- Tensile test curves shown increasing of UTS and ductility by elevation of friction presssure and due to used of high rotation speed led to increases of UTS,
- SEM observation seemed the degree of thermo-plastic deformation according to the amount of spiral forms, that result of aggressive friction pressure at elevated temperature and high rotation. Whilst, magnification of central region of fracture seems most ductile mode with micro-porocities of different forms and dimensions. This mode of ductile fracture seems more clear at 170 MPa,
- XRD analysis exposed the concentration of FCC structure of gamma iron at level of 111 due to thermomechanical strain at high rotation speed and aggressive friction pressure application. Thus, Mo element effects on the cooling rate which give it ability to effect on the phase attentiveness in the welding joint,
- Concerning the grade AISI 316, increasing of friction pressure (170 MPa) with high rotation speed (3000 rpm) cause elevated temperature (1057 °C), which lead to high level of hardness and micro-hardness at the interface, and also elevation in UTS and ductility. On the other hand, low friction pressure provides poor properties of welding joint.

5. REFERENCES

1. Titouche, N., Boukharoubab, T., Amzert, S., Hassan, A. J., Lechelalah, and R., Ramtani, S., Direct Drive Friction Welding Effect on Mechanical and Electrochemical Characteristics of Titanium Stabilized Austenitic Stainless Steel (AISI 321) Research Reactor Thick Tube, *Journal of Manufacturing Processes*, Vol. 41 (2019), 273-283, <https://doi.org/10.1016/j.jmapro.2019.03.016>.
2. Hincapié, O. D., Salazar, J. A., Restrepo, J. J., Torres, E. A., and Graciano-Urbe, J., Control of Formation of Intermetallic Compound in Dissimilar Joints Aluminum-steel, *International Journal of Engineering , Transactions B: Applications*, Vol. 32, No. 1, (2019), 127-136, doi: 10.5829/ije.2019.32.01a.17.
3. Hamdan, A. I., Stress Concentration Factors (SCFs) in Circular Hollow Section CHS-to-H-shaped Section Welded T-Joints under Axial Compression, *Civil Engineering Journal*, Vol. 5, No. 1 (2019), 33-47, <http://dx.doi.org/10.28991/cej-2019-03091223>.
4. André, S. J., Douglas, M., Vieira Braga, L. G., Afonso, R., and Dornelles, R. F., Replacement of Gas metal arc welding by friction welding for joining tubes in the hydraulic cylinders industry. *Materials Research*, 21, No. 4. (2018), <https://doi.org/10.1590/1980-5373-MR-2018-0015>.
5. Peng, L., Jinglong, L., Muhammad, S., Li, L., Jiangtao, X., and Fusheng, Z., Effect of Friction Time on Mechanical and Metallurgical Properties of Continuous Drive Friction Welded Ti6Al4V/SUS321 Joints, *Materials and Design*, Vol. 56, (2014), 649-656, <http://dx.doi.org/10.1016/j.matdes.2013.11.065>.
6. Hassan, A.J., Boukharouba, T., Miroud, D, and Ramtani, S., Metallurgical and Mechanical Behavior of AISI 316- AISI 304 during Friction Welding Process, *International Journal of Engineering , Transactions B: Applications*, Vol. 32, No. 2, (2019), 284-291, doi:10.5829/ije.2019.32.02b.16.
7. Ethiraj, N., Sivabalan, T., Sivakumar, B., Vignesh Amar, S., N. Vengadeswaran, and Vetrivel K., Effect of Tool Rotational Speed on the Tensile and Microstructural Properties of Friction Stir Welded Different Grades of Stainless Steel Joints, *International Journal of Engineering , Transactions A: Basics*, Vol. 33, No. 1, (2020), 141-147, doi: 10.5829/ije.2020.33.01a.16.
8. Villegas, J.F., Guarín, A.M., and Unfried-Silgado, J., A Coupled Rigid-viscoplastic Numerical Modeling for Evaluating Effects of Shoulder Geometry on Friction Stir-welded Aluminum Alloys, *International Journal of Engineering, Transactions B: Applications*, Vol. 32, No. 2, (2019), 184-191, doi: 10.5829/ije.2019.32.02b.17.
9. Hasanzadeh, R., Azdast, T., Doniavi, A., Babazadeh, S., Lee, R. E., Daryadel, M., and Shishavan, S. M., Welding Properties of Polymeric Nanocomposite Parts Containing Alumina Nanoparticles in Friction Stir Welding Proces, *International Journal of Engineering Transactions A: Basics*, Vol. 30, No. 1, (2017), 143-151, doi: 10.5829/idosi.ije.2017.30.01a.18.
10. Singh, R., Rizvi, S. A., and Tewari, S. P., Effect of Friction Stir Welding on the Tensile Properties of AA6063 Under Different Conditions, *International Journal of Engineering. Transactions A: Basics*, Vol. 30, No. 4, (2017), 597-603, doi: 10.5829/idosi.ije.2017.30.04a.19.
11. Shishavan, S. M., Azdast, T., Aghdam, K. M., Hasanzadeh, R., Moradian, M., and Daryadel, M., Effect of Different Nanoparticles and Friction Stir Process Parameters on Surface Hardness and Morphology of Acrylonitrile Butadiene Styrene, *International Journal of Engineering Transactions A: Basics*, Vol. 31, No. 7 , (2018), 1117-1122, doi: 10.5829/ije.2018.31.07a.16.
12. Muralimohan, C.H., Muthupandi, V., and Sivaprasad, K., Properties of Friction Welding Titanium-Stainless Steel Joints with a Nickel interlayer, *Procedia Material Science*, Vol. 5, (2014), 1120-1129, <https://doi.org/10.1016/j.mspro.2014.07.406>.
13. Handa, A., and Chawla, V., Mechanical Characterization of Friction Welded Dissimilar Steels at 1000 rpm, *Materials Engineering*, Vol. 20, (2013), 102-111, <http://fstroj.uniza.sk/journal-mi/PDF/2013/14-2013.pdf>.

14. Ma, H., Qin, G., Geng P., Li, F., Fu, B., and Meng, X., Microstructure Characterization and Properties of Carbon Steel to Stainless Steel Dissimilar Metal Joint Made by Friction Welding. *Materials and Design*, Vol. 86, (2015), 587-597, <https://doi.org/10.1016/j.matdes.2015.07.068>.
15. Hassan, A.J., Boukharouba, T., and Miroud, D., Characterizations of Friction Welding Joint Interface for AISI 316, *China Welding*, Vol. 28, No. 1, (2019), 42-48, doi: 10.12073/j.cw.20180811001.
16. Ajith, P. M., Afsal Husain, T. M., Sathiya, P., and Aravindan, S., Multi-objective Optimization of Continuous Drive Friction Welding Process Parameters Using Response Surface Methodology with Intelligent Optimization Algorithm, *Journal of Iron and Steel Research, International*, Vol. 22, No. 10, (2015), 954-960, [https://doi.org/10.1016/S1006-706X\(15\)30096-0](https://doi.org/10.1016/S1006-706X(15)30096-0).
17. Hassan, A.J., Lechelah, R., Boukharouba, T., Miroud, D., Titouche N., and Ouali N., History of Microstructure Evolution and its Effect on the Mechanical Behavior During Friction Welding for AISI 316, Edts. T. Boukharouba; et al., *Springer International Publishing Switzerland*, (2017), 51-65, http://doi:10.1007/978-3-319-41468-3_5.
18. Kimura, M., Kusaka, M., Kaizu, K., Nakata K., and Nagatsuka K., Friction Welding Technique and Joint Properties of Thin-Walled Pipe Friction Welded Joint Between Type 6063 Aluminum Alloy and AISI 304 Austenitic Stainless Steel, *International Journal of Advanced Manufacturing Technology*, Vol. 82, (2016), 489-499, <https://doi.org/10.1007/s00170-015-7384-8>
19. Ajith, P.M., Barik, B. K., Sathiya, P., and Aravinda S., Multiobjective Optimization of Friction Welding of UNS S32205 Duplex Stainless Steel, *Defence Technology*, Vol. 11, (2015), 157-165, <https://doi.org/10.1016/j.dt.2015.03.001>.
20. Alves, E. P., Neto, F. P., An, C. Y., and Castorino da Silva E., Experimental Determination of temperature During Rotary Friction Welding of AA1050 Aluminum with AISI 304 Stainless Steel. *Journal of Aerospace Technology and Management*, Vol. 4, No.1, (2012), 61-67, doi 10.5028/jatm.2012.04013211.
21. Kirik, I., and Ozdemir, N., Weldability and Joining Characteristics of AISI 420/AISI 1020 Steels using friction welding, *International Journal of Materials Research*, Vol. 104, No. 8, (2013), 769-775, <https://doi.org/10.3139/146.110917>.
22. Khidhir, G. I., and S. A. Baban, Efficiency of Dissimilar Friction Welded 1045 Medium Carbon Steel and 316L Austenitic Stainless Steel Joints, *Journal of Materials Research and Technology*, Vol. 8, No. 2, (2019), 1926-1932, <https://doi.org/10.1016/j.jmrt.2019.01.010>.
23. Liu, F.C., and Nelson, T.W., Twinning and Dynamic Recrystallization in Austenitic Alloy 718 During Friction Welding, *Material Characterization*, Vol. 140, (2018), 39-44, <https://doi.org/10.1016/j.matchar.2018.03.035>.
24. Kaushik, N., and Singhal, S., Experimental Investigations on Microstructural and Mechanical Behavior of Friction Stir Welded Aluminum Matrix Composite, *International Journal of Engineering, Transactions A: Basics*, Vol. 32, No. 1, (2019), 162-170, doi: 10.5829/ije.2019.32.01a.21.

Persian Abstract

چکیده

این مطالعه بر روی تأثیر فشار اصطکاک بر مقاومت اتصال جوشکاری AISI 316 متمرکز است. برای ارزیابی تأثیر فشار اصطکاک از روش تک عاملی استفاده شد، در حالیکه سایر شرایط ثابت نگه داشته می شوند. داده های تجربی با اندازه گیری دما با استفاده از دماسنج مادون قرمز و دماسنج با لمس، جایی که سختی Hv10 و میکروسختی Hv0.1 در امتداد جهت محوری، نمونه آزمایش کششی با قطر موثر ۸ میلی متر، میکروسکوپ الکترونی روبشی (SEM) برای مشاهده کشش به دست آمد، به دست آمد. سطح شکستگی و پراش اشعه ایکس (XRD) برای تجزیه و تحلیل غلظت آهن گاما. نتایج حاصل از فشار اصطکاک بالا، افزایش دما در مرحله اصطکاک و جعل، مقادیر سختی و ریز سختی بالا در مرکز جوشکاری، شکل پذیری بهبود یافته و مقاومت کششی نهایی (UTS) را فراهم می کند. در حالی که ناحیه مرکزی شکستگی کششی به نظر می رسد بیشتر حالت شکل پذیری و وجود ریز تخلخل ها با اشکال و ابعاد مختلف باشد، از این رو غلظت ساختار مکعب صورت محور (FCC) آهن گاما به وضوح در سطح ۱۱۱ نشان داده شده است.
